NACA

RESEARCH MEMORANDUM

AN AIR-BORNE TARGET SIMULATOR FOR USE WITH SCOPE-

PRESENTATION TYPE FIRE-CONTROL SYSTEMS

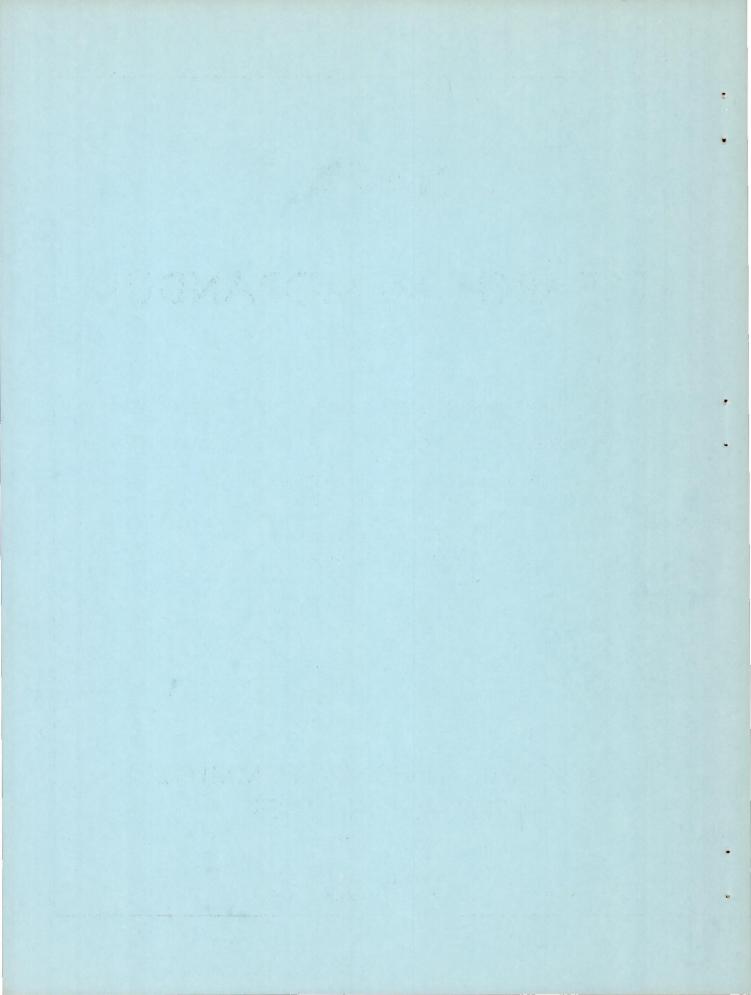
By John V. Foster, Elmer C. Fulcher, and Donovan R. Heinle

Ames Aeronautical Laboratory Moffett Field, Calif.

NATIONAL ADVISORY COMMITTEE FOR AERONAUTICS

WASHINGTON

May 10, 1957 Declassified September 1, 1961



NATIONAL ADVISORY COMMITTEE FOR AERONAUTICS

RESEARCH MEMORANDUM

AN AIR-BORNE TARGET SIMULATOR FOR USE WITH SCOPE-

PRESENTATION TYPE FIRE-CONTROL SYSTEMS

By John V. Foster, Elmer C. Fulcher, and Donovan R. Heinle

SUMMARY

The design and flight evaluation of an air-borne target simulator using precomputed relative kinematics for use in tracking studies of fighter aircraft equipped with scope-presentation type fire-control systems are described.

Experience showed the desirability of a target simulator which would be air-borne to provide normal stimuli to the pilot, provide standard repeatable attacks for comparative studies, and eliminate problems associated with target aircraft. Preliminary design studies indicated that a simulator using programmed precomputed relative kinematic data would be satisfactory for portions of the tracking research.

The simulator was installed in an F86-D airplane equipped with a Hughes $E-\mu$ fire-control system. A flight program was conducted to evaluate the performance of the equipment. The evaluation, based primarily on pilot opinion, disclosed that the simulator duplicated the attack phase of a normal $E-\mu$ system run. It appeared that the simulator might be applied to other problems than tracking research, such as pilot training.

INTRODUCTION

Flight programs involving research on target tracking with fightertype aircraft have been conducted by the Ames Aeronautical Laboratory for
some years. With earlier programs the primary purpose of this type of
research was to provide information of value in the design of effective
fighter aircraft. Recent programs have in addition been aimed toward providing information for the design of automatic air-borne fire-control
equipment with emphasis on design for optimum compatibility with the aircraft. This compatibility factor has assumed an increasingly important
role, especially where the fire-control system ties directly to the
aircraft control surface system.

Flight studies have been made which investigated the tracking problems associated with various types of optical sights and radar fire-control systems. Progressively, programs have been run with fixed, or "iron" sights, disturbed recticle sights, such as the A-1, scope-presentation fire-control systems - in particular, the Hughes E-4 fire-control system, and currently, systems with a tie-in to the aircraft controls.

Unfortunately, flight measurements are not conducted under precisely repeatable laboratory type conditions; hence, performance differences due to system improvement tend to be obscured by changes in flight conditions between runs. In order to achieve repeatable target runs consideration was given to a device which would eliminate the use of an actual target and substitute a programmed artificial target. Such a device would provide a means of programming identical target runs as often as required. This would greatly facilitate comparative analysis of tracking performance resulting from system or aircraft changes which might otherwise be obscured by variations in attack geometry. In addition, the flight program could be considerably accelerated by the elimination of several timeconsuming factors inherent in conventional tracking methods. These factors include: the excessive number of runs and associated data reduction necessary to produce and identify runs similar enough to make comparative studies; the accurate positioning of the fighter and target prior to an actual run; the between-flight delays involved in coordinating flights with a target airplane. In the case of the scope-presentation-type firecontrol system, the additional delays associated with "lock-on" problems would be eliminated as well as the very real danger of collision.

Since the Laboratory was primarily interested in research conducted during the final precise tracking portion of the over-all mission, it was decided to simulate only that period after the target had been aligned in the sight, or "locked-on" in the case of the scope presentation systems. The function of the simulator from that point on would be to establish a test problem which would allow precise measurement of the test parameter deviations while realistically duplicating a real target run. It would be essential that the simulator be air-borne in order to include all stimuli to which the pilot normally responds; furthermore, as much of the real sight or fire-control system as possible should be used.

The Laboratory's first exploration in this direction was a simulator for use with an optical gunsight, constructed and evaluated at Ames and described in reference 1. As a logical continuation of the Ames tracking research utilizing optical gunsights, the Laboratory proceeded to a study of a radar-tracking, scope-presentation, fire-control system - more particularly, the E-4 fire-control system in an F86-D airplane. In view of the encouraging experience with the original optical-gunsight target simulator, it appeared desirable to develop functionally similar equipment for use with this more advanced type of fire-control system. The development of this target simulator for a scope-presentation fire-control system and the results of a brief series of flight tests are presented herein.

NOTATION

A	antenna angle in azimuth, radians
An	normal acceleration, g's
В	relative bearing of attacker from bomber path, radians
E	antenna angle in elevation, radians
F	relative rocket travel, yd
LS	line of sight from attacker to target
R	target range, yd
Ř	target range rate, yd/sec
T	time-to-go until impact, sec
v_A	interceptor velocity, yd/sec
v_B	target velocity, yd/sec
t	time, sec
θ	target azimuth angle relative to attacker flight path, radians
λ	flight path angle, radians
φ	bank angle, radians
ω	angular velocity of antenna, radians/sec
	Cubaccinta

Subscripts

D azimuth

E elevation

R radar line of sight

Superscripts

- about banked control-line axis
- " about unbanked control-line axis

Axes Systems

X,Y,Z interceptor wind axes

SIMULATOR DESIGN

Preliminary investigation of the target simulator concept produced various possible designs capable of reproducing the attack phase. As an example, one design would combine programmed target kinematics with measured attacker kinematics as illustrated in figure 1. Indications were, however, that a more limited type of simulator of much greater simplicity would meet the requirement of a considerable part of the Ames research. As a result of this preliminary investigation a type of simulation which uses precomputed relative kinematics was decided on.

To understand properly the target simulator design, one should first understand the basic principles of the Hughes E-4 fire-control system. A simplified functional block diagram of the E-4 is illustrated in figure 2(a). For those not familiar with this particular system, additional information is contained in Appendix A and a complete description is contained in reference 2. A functional block diagram showing the E-4 system with target simulator components added is illustrated in figure 2(b).

Simulated Quantities

A target simulator must provide the functions normally supplied by the self-tracking radar, that is, it must have provision for locking on the simulated target in space; it must drive the antenna so as to keep it pointed at the simulated target in spite of own-ship motions; and it must allow the computer and the pilot's display to operate in the normal fashion.

To provide these functions the target simulator must substitute information normally supplied by the radar circuits. This information basically consists of target range, line-of-sight angles, and

line-of-sight angular rates. In the E-4 system this information is obtained by the radar which samples the present target position and compares it with the previous position so as to generate range and line-of-sight direction error signals. The line-of-sight error signal is proportional to the angular rate of the line of sight (line-of-sight rate) of the target relative to the attacker, and is used as such, both as an input to the data computer and as an input to the antenna drive system. This fact leads to a very convenient method for simulating a true target in which programmed signals may be substituted for the normal inputs.

The computer processes the data from the radar according to definite equations in order to present a steering signal to the pilot. If the pilot flies with no tracking error, the aircraft flight path can be computed for a given target maneuver and given initial conditions by using the steering equations. From this computed flight path, the line-of-sight rates and the target range can be calculated as a function of time during the attack. These relative kinematics data are used as the target simulator programmed input.

Line-of-Sight Rate Programming

The method of antenna positioning used by the E-4 utilizes two single-degree-of-freedom integrating gyro units (HIGU) mounted on the antenna, perpendicular to each other and to the line of sight. These gyro axes are fixed to the antenna which is gimballed to the airframe; hence, they will assume some bank angle dependent both on aircraft roll attitude and antenna position. The radar system is designed to supply the line-of-sight error signals in components about these banked antenna axes. For the target simulator, it was not considered feasible to precompute and program the line-of-sight rates directly in these banked antenna coordinates because of the difficulty arising from the short-term variations in bank angle during an attack. Although these variations do not materially affect the flight path or the line-of-sight rates in unbanked coordinates, they do seriously affect any rates programmed in banked antenna axes. As a result, it was necessary to program the lineof-sight rates in unbanked axes perpendicular to a known control line and to process the data further to obtain the rates in banked antenna axes.

The method chosen utilized programmed rates about unbanked axes perpendicular to a reference control line as the basic input and transformed these rates into banked antenna rates. The reference control line chosen was the unbanked aircraft flight path center line. The line-of-sight rates were first converted to rates about banked axes perpendicular to the control line, and then to rates about the banked antenna axes perpendicular to the line of sight. This last transformation placed the rates in the correct axes for driving the antenna.

A discussion of the axes-transformation equations and the computer which was mechanized to perform the transformation is included in Appendix B.

Range and Range-Rate Programming

The range information was stored in a programmer and supplied to the system simultaneously with the line-of-sight rate information. For convenience, the calculated range-rate was also programmed. Normally, the system generates range-rate information by differentiating the range signal. This procedure, however, tends to magnify any noise on the input signals; consequently, the range programming would have to be extremely smooth to produce a reasonably clear range-rate signal. In practice it was found easier to program the range-rate signal.

The details of program layout, both in range and line-of-sight rates, are covered in Appendix C.

Noise Simulation

One difference between real and synthetic line-of-sight rate signals is the lack of noise due to the target scintillation and other causes normally contributed by the radar. Since the programmed line-of-sight rate signals contained no noise, the introduction of artificial noise into the steering signals was necessary.

CONSTRUCTION AND INSTALLATION

Simulator Components

Aside from instrumentation, the target simulator equipment consisted of three separately packaged units. These were the programmer, the axestransformation computer, and the noise generator.

The programmer supplied azimuth line-of-sight rate, elevation line-of-sight rate, range and range-rate signals to the E-4 system by means of motor driven cams (fig. 3). The axes transformation computer transformed the line-of-sight rate signals from rates about the unbanked control line axes to rates about banked antenna axes (fig. 4).

The noise generator produced signals with an amplitude and frequency spectrum similar to the steering dot noise from a real target, at the same point in the system. Different noise signals were supplied to the

horizontal and vertical steering dot components in order to prevent any correlation between the horizontal and vertical dot motion. The equipment consists of a constant-speed motor which drives an endless belt of film past two slots, behind each of which is a special long-filament bulb (fig. 5). On the film is a partially blacked record which, when driven at the correct speed, produces a signal corresponding to the desired noise spectrum. The film varies the light to a photo tube which produces the desired noise signal.

Simulator Signal Flow

The signal flow of the programmed quantities may be followed by reference to figure 6. The four signals ω_E ", ω_D ", R, and R are generated in the programmer. The two rate signals ω_E " and ω_D " pass from the programmer through the axes transformation computer to the regular E-4 system gyro-torque generators. The range signal R is introduced at the input of the range servo and the time servo; the range-rate R is introduced at the range-rate amplifier output. From these points on, the operation is the same as for real targets.

Aircraft Installation

Major components of the target simulator were installed in the nose hatch cover of the test aircraft (fig. 7). This location served the dual function of providing accessible mounting in an otherwise crowded airplane and allowed removal of the complete simulator equipment for servicing in the laboratory. Furthermore, the aircraft could be flown for other tests during servicing periods by using a spare nose hatch cover.

Tie-ins to the E-4 circuits were primarily made by the use of "tee-type" cables which avoided cutting into the original E-4 system cables. All of the connections to the E-4 were controlled by relays in the target simulator in such a manner as to allow the pilot to switch from normal E-4 operation to target simulator operation at will. The target simulator cockpit controls are shown in figure 8.

INSTRUMENTATION

The instrumentation used was of three different types: cockpit indicators, recorded functions, and a telemetered scope display.

Two cockpit indicators presented readings proportional to the steering dot errors integrated over the last 10 seconds of each run. These

readings were generated by rectifying each steering dot signal and using these rectified signals to drive precise integrating motors during the integration period. Separate indicators were used for the elevation and azimuth channels (fig. 8). Another cockpit indicator presented the time required, from the program start, for the pilot to bring the steering dot inside the reference circle.

A cockpit camera was used to make 16 mm moving picture records of the pilot's scope display during the simulated attacks.

A small ll-channel recording oscillograph was used to record quantities of interest. Figure 9 illustrates samples of the records. The actual records were made on color film to aid trace identification.

A telemeter installation was used to allow simultaneous ground viewing of the pilot's scope during the attack runs, and proved to be quite useful in the simulator development. The relatively small number of airborne components required to transmit the scope signals made for a simple installation, since a standard FM/FM telemeter receiving station was available.

The nature of the attack display of the E-4 is such that the various signals to produce the steering dot, artificial horizon, reference circle, time-to-go, etc., are commutated in the system by a series of relays so as to present the individual pieces of information to the pilot's cathoderay tube scope in a time sequence. The pilot actually sees all the information simultaneously because of scope and eye persistence. Thus, many signal sources are commutated into only the three separate signals necessary to operate the attack gun of the display scope: vertical deflection, horizontal deflection, and intensity. This circumstance greatly simplifies the telemetering problem. Rather than telemeter the many individual computer signals and commutate at the ground station, in order to reproduce the pilot's scope pattern, it is only necessary to transmit these three signals. After demodulation at the ground station, the signals are supplied to the horizontal, vertical, and intensity inputs of the ground observer's scope to reproduce the same attack display the pilot is viewing. In addition to simplifying the equipment, the use of the three commutated signals insures that the various display items will appear in the proper relation to each other, the prime requirement in interpreting and using the ground scope. The ground display equipment is illustrated in figure 10.

FLIGHT TESTS

Flight Test Objectives

The equipment was installed in an Air Force F86-D airplane for the purpose of flight tests which were directed more toward qualitative

evaluation than toward extensive quantitative documentation. The method of quantitative evaluation used previously for the optical target simulator (ref. 1), in which results of attacks against the simulated target are compared to similar attacks against an actual target, was not considered warranted in the present case, primarily because of the time and effort involved in making the required numerous and carefully controlled attacks against an actual target. In general, the development program depended heavily on pilot opinion to point out deficiencies. The instrument records were utilized to understand the difficulties and devise corrective changes. Concurrent programs on other aircraft utilizing the E-4 system provided the pilots with experience which made them cognizant of details such as noise, steering dot dispersion, and system response. This circumstance greatly enhanced the value of the pilot's opinions regarding the performance of the simulator as compared to operations against real targets.

The pilot could select any of three different attacks incorporated in the programmer. He also had the choice of programming the runs to the right or to the left, with or without noise. Although noiseless runs are unrealistic and of questionable value in pilot training, they are of use in certain types of research.

A typical run consisted of the following steps. The pilot, by means of the hand control, directed the antenna toward the target initial position and then released the action switch, whereupon the system switched to the locked-on automatic tracking condition. From this point on, the pilot completed the attack in the normal fashion.

Simulator Evaluation

Two basic simulator operations checked in flight were the proper transformation of the space programmed line-of-sight rates into appropriate antenna coordinate line-of-sight rates, and proper correlation of the programmed line-of-sight rates, range, and range rate to produce the correct flight path.

Incorrect angular rate transformation resulted in the programmed azimuth rate affecting the elevation rate and, consequently, the altitude as illustrated in figure 11. Incorrect correlation of programmed quantities resulted in a curved flight path, as illustrated in figure 12, instead of the precomputed straight flight path. These problems were satisfactorily resolved during the flight program.

Evaluation by Air Force Pilots

During the flight tests, the Laboratory received valuable assistance from the Interceptor Pilot Research Laboratory at Tyndall Air Force Base. On two occasions, once near the start of the flight tests and once near the completion, the IPR Laboratory sent experienced E-4 pilots to make a preliminary flight evaluation of this equipment with regard to potential usefulness as an aid to interceptor pilot training. The comments of these visiting pilots were highly regarded and proved to be of considerable assistance in the development program.

DISCUSSION

Pilots and engineering personnel considered the simulation of the attack phase to be quite realistic once the shakedown flights had been completed. The simulator had several characteristics desirable for research and training: Many runs could be duplicated in a relatively brief period of time; specific types of attacks could be easily programmed; studies could be made of the effects of noise, or the lack of noise in tracking performance; target aircraft could be eliminated, resulting in savings of research pilot and aircraft time and eliminating the ever present possibility of collision.

The ability to repeat selected attack conditions quickly and accurately is of particular value in comparative studies. Such studies include comparison of the effects of aerodynamic changes, optimum attack display studies, pilot training and evaluation.

Relative Kinematic Programming Considerations

Although the type of programming used for this simulator was satisfactory for conducting certain research on the attack phase of the firecontrol problem, it may have certain limitations in other uses. These limitations introduce problems which may be of interest to others concerned with different phases of the interceptor task. The problems include those connected with flight path deviations, target acquisition procedure, and programming layout.

Flight-path deviations. - Problems associated with deviations from the precomputed flight path arise because the relative line-of-sight rates and ranges are computed from a predicted attacker flight path and the pilot must fly this same flight path if the attack pattern is to be exactly as precomputed.

Short term variations arise from the pilot's inability to track precisely enough to keep the dot exactly centered and from changes in steering commands due to radar system noise. These variations cause only minor deviations from the precomputed flight path because they tend to fluctuate in all directions, canceling their own effects on the mean flight path. Furthermore, it should be noted that while these short term oscillations may cause changes in aircraft attitude, the corresponding changes in the velocity vector, or flight path direction, are relatively small. Since the system is space-stabilized, the attitude variations are not important; it is only the considerably smaller flight-path variations that affect simulation accuracy.

Long term flight path deviations would arise if the pilot chose to fly some path other than that called for by the steering dot. Since, in tracking research, the pilots were instructed to fly the commanded steering signal course, these large deviations did not arise. They could be of considerable importance, however, in pilot training where tactical considerations may cause the pilot to deviate from the computed course.

Target acquisition. For research tracking studies, it is not necessary to have the target acquisition phase incorporated in the simulator. Nevertheless, the method used for initiating a simulated attack was quite similar to standard E-4 procedure except that lock-on was always achieved, range gate manipulation was not required, and initial target angle was specified to correspond to a particular program. In practice, it was found advantageous to allow the pilot certain freedom in setting the initial target angle since the system made the necessary adjustments to the initial turn as it would have with a real target. This feature resulted in increasing the variety of attack patterns.

Program layout. The difficulties associated with program layout arose from line-of-sight rate scale factors and minor terms in the elevation steering equations. The scale factor problem arose because of the large ratio between programmed line-of-sight rates at the firing point and the rates during the early portion of the attack. This ratio may be 100 to 1 or greater. Since the sine of the azimuth steering angle called for is directly proportional to the azimuth line-of-sight rate, a 10-percent angle accuracy at the extremely low rates might require 0.1 percent accuracy of programmed full scale rates. This problem was overcome by using two rate cams having mechanical scale factors which differed by a ratio of 10 to 1. At an appropriate point during the run the program was switched from one cam to the other and, simultaneously, a change of electrical scale factor was made to offset precisely the change of mechanical scale factor.

The problems in elevation line-of-sight rate programming were primarily due to the minor terms associated with the rocket trajectory. Another factor which restricted elevation rate programming was that the axes transformation computer was limited because of an assumption made

in deriving the equations (Appendix B). As a result of these considerations, all of the flight tests were made with programmed zero vertical motion. It was realized that this did not precisely represent the actual case, even against a nonmaneuvering target, because of certain minor terms in the elevation-steering equations. In view of the possibility of difficulties in correctly programming elevation rates, it was thought easier to program zero elevation rate and take care of the minor terms by other methods.

Restrictions To System Evaluation

Although the simulator could be used in testing certain aspects of the fire-control system itself (e.g., attack data presentation methods), caution must be exercised in this type of application. The simulator does not use the complete fire-control system; furthermore, such things as noise are artificially introduced near the output of the system. Changes within the system, such as filter time constants, would not be properly indicated by corresponding changes in steering dot noise.

Another, and possibly more serious, limitation results from the fact that the outer kinematic loop, which includes the attacker, target, and connecting radar radio-frequency link, is eliminated. Normal radar system operation provides a feedback of information from this loop, whereas with the target simulator this particular information is lacking. To visualize the effect consider a case where a sudden pitching of the attacker is partially conveyed to the antenna. The antenna stabilization system will attempt to prevent the antenna from following the aircraft motion; however, it may momentarily fail to do so because of limited dynamic response. During this period when the antenna is not maintaining perfect stability the effects are quite different between the real and simulated target cases. In the real target case, the beam is displaced from the target; consequently, the radar feeds information back to the system, indicating this displacement. Such is not the case with a simulated target since the radio-frequency link is not used. Normally this difference is of little consequence; however, under certain circumstances with a real target, the combination of this outer loop and other system loops can cause an unstable condition resulting in loss of lock-on. It is apparent that for studies concerned with such questions of stability, this target simulator would fail to produce the necessary conditions.

CONCLUDING REMARKS

An air-borne target simulator offers many desirable features for tracking research and pilot training without eliminating the sensory inputs to which the pilot responds.

The flight program demonstrated that a simple type of target simulator using programmed relative kinematics information is capable of producing quite realistic attacks. This conclusion is substantiated primarily by pilot opinion. The limited amount of instrument data obtained verifies this opinion although no detailed quantitative comparison with actual target runs was attempted.

The simulator produces standard repeatable attack patterns for comparison studies of the effects of changes in aircraft or fire-control system display parameters. It also eliminates the target airplane with its time consuming operational problems, lock-on difficulties, and collision danger.

The same advantages also appear important for other applications, such as pilot training and evaluation. Particularly desirable features for this use are the ability to produce many attacks during a brief flight, score the tracking performance, and avoid collision dangers. Furthermore, the simplicity allows installation without interfering with the normal system so that the pilot can freely switch from real target operation to simulated target operation during flight.

The programmed relative kinematics type of simulator is satisfactory for certain tracking research but the method has limitations which become important as more aspects of the complete attack are incorporated.

Ames Aeronautical Laboratory
National Advisory Committee for Aeronautics
Moffett Field, Calif., Mar. 19, 1957

APPENDIX A

THE E-4 FIRE-CONTROL SYSTEM OPERATION

Examination of a simplified functional block diagram of the E-4 fire-control system (fig. 2(a)) discloses that the system consists of five rather distinct functional groups. A brief description of these groups is given below for those not familiar with the E-4 system.

The first group, the radar, consists of the radio frequency portion which includes, among other things, the transmitter, receiver, and timing circuits. It is used to detect the target, locate its direction, and determine its range. A further function of this group is to detect changes in the position of the target and supply a corrective signal to the drive circuits so as to keep the antenna pointed at the target.

The second group, the antenna drive and space-stabilization circuits, serves a twofold purpose. First, it provides a means of stabilizing the antenna against own-ship motions, and secondly, when proper radar tracking error signals are introduced, it provides a means of precisely turning the antenna at the rates necessary to keep it pointed at the target.

The method of stabilizing and driving the antenna by the use of two single-degree-of-freedom, hermetically sealed, integrating rate-gyros (HIGU) is adequately covered in references 2 and 3. Briefly, the system operation is as follows. The two integrating gyro units are rigidly fixed to the antenna with their input axes parallel to the antenna elevation and deflection axes, respectively. The HIGU integrates the difference between the true rate of antenna rotation, sensed from the gyro precessional torque, and the desired rate of rotation, represented by an externally applied torque signal. When the applied torque signal is zero, any disturbance tending to cause rotation of the antenna is sensed by the HIGU. The HIGU output signal is fed through an amplifier to a motor which drives the antenna at the correct angular velocity with respect to the airplane to cause zero antenna rotation in space. Thus the antenna provides a stabilized reference axis. When a torque signal is applied to the HIGU, the resulting output signal causes the drive motor to rotate the antenna at an angular velocity in space sufficient to produce precessional torque to balance the applied torque exactly, resulting in an angular velocity proportional to the applied signal. In normal E-4 operation the radar tracking error signal generates the necessary signal to drive the antenna, whereas, in the target simulator, the necessary rates are obtained by programming the applied torque signals. The integrating feature of the HIGU assures that the antenna will rotate through an angle equal to the time integral of the desired rate, regardless of dynamic lags in the system.

The third group, the data computer, uses the information from the previously described groups to compute steering information for the pilot. It uses the range information and the line-of-sight rates from the radar information unit, together with angle resolvers on the antenna, to compute steering information for the pilot's display.

The fourth group, the pilot's scope display, gathers the results of the computer and presents the data in a form suitable for the pilot's guidance. In addition to steering dot, range, range-rate, and time-to-go information, it presents an artificial horizon and an indication of the target's relative bearing in azimuth.

The fifth group, the firing group, processes ballistics data and information from the data computer to operate the rocket firing mechanism and give the collision pull-out signal.

APPENDIX B

TARGET SIMULATOR DESIGN

Relative Kinematic Programming

The target simulator operated on the basis of programmed precomputed relative kinematic data in the form of azimuth line-of-sight rate, elevation line-of-sight rate, range, and range rate of the simulated target, all relative to the attacker's assumed control line reference. This control line reference corresponded to the predicted attacker flight path center line. Since the E-4 system required the line-of-sight rate signals to be supplied in components about the banked antenna axes, a transformation had to be made from unbanked airplane or control line axes to banked antenna axes.

The simplest method of transferring the programmed line-of-sight rates to the proper axes would have been to make a direct axes transformation by passing the signals through a resolver, set to the correct angle by a roll gyro mounted on the antenna. This method was used on the optical target simulator described in reference 1. In the case of the E-4 system, no roll gyro could be found which was small enough to be mounted on the antenna and yet cause no interference with normal radar operation and antenna stabilization. Accordingly, an alternate method using an axes transformation computer was devised.

Equations, which are developed below, showed that the axes transformation could be made with a relatively simple computer. While the transformation is not precisely correct, the error is small under the conditions used.

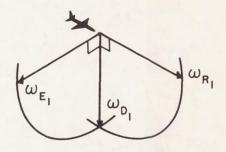
Transformation Equations

The equations developed below are for the purpose of converting programmed line-of-sight rates in axes perpendicular to an unbanked control line to rates about banked antenna axes. The transformation is best considered in two parts; first, from rates about the unbanked control line axes to rates about the banked control line axes; and secondly, from these resultant rates about the banked control line to rates about the banked antenna axes. This procedure may be visualized by considering the aircraft to be initially flying a straight and level course with the antenna pointed straight ahead so that the R, E, and D axes of the antenna coincide with the X,Y,Z axes of the aircraft. In the first step the aircraft is banked about the X axis (coincident with the initial position of the R axis) through the angle φ . The second step

consists of turning the antenna about its azimuth axis through the angle A and then about its elevation axis through the angle E until the R axis of the antenna points along the line of sight to the target. Note that the X axis of the aircraft has been assumed to coincide with the control line.

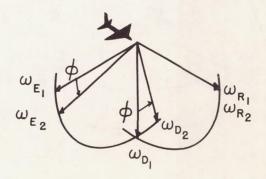
For the purpose of developing the transformation, the following subsubscripts are added to conform to the set of axes under consideration; for example, the first step goes from axes R_1, E_1, D_1 to axes R_2, E_2, D_2 .

The programmed unbanked rates are illustrated by the following sketch.



Axes set No. 1

First bank the axis about $~\omega_{R_1}~$ by roll angle $~\phi~$ to obtain banked control line rates $~\omega_{E_2}$ and $~\omega_{D_2}$.



Axes set No. 2

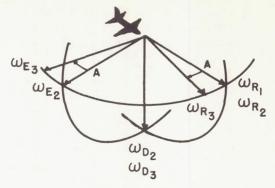
where

$$\omega_{E_2} = \omega_{E_1} \cos \varphi + \omega_{D_1} \sin \varphi$$
 (B1)

$$\omega_{D_2} = \omega_{D_1} \cos \varphi - \omega_{E_1} \sin \varphi$$
 (B2)

This completes the first part of the transformation. The second part will be concerned with converting the banked control line rates $\omega_{\rm E_2}$ and $\omega_{\rm D_2}$ into banked antenna axes.

Move the antenna in azimuth through angle A as follows,



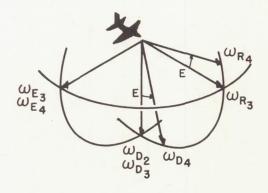
Axes set No. 3

where

$$\omega_{R_3} = \omega_{R_1} \cos A + \omega_{E_2} \sin A$$
 (B3)

$$\omega_{E_3} = \omega_{E_2} \cos A - \omega_{R_1} \sin A$$
 (B4)

Then move the antenna in elevation through angle E.



Axes set No. 4

where

$$\omega_{R_4} = \omega_{R_3} \cos E - \omega_{D_2} \sin E$$
 (B5)

$$\omega_{D_4} = \omega_{D_2} \cos E + \omega_{R_3} \sin E$$
 (B6)

For the programs contemplated, it was assumed that $\omega_{R_4} = 0$. Then from equation (B5):

$$\omega_{R_3} = \omega_{D_2} \frac{\sin E}{\cos E}$$
 (B7)

and from equations (B6) and (B7):

$$\omega_{D_4} = \omega_{D_2} \cos E + \omega_{D_2} \frac{\sin E}{\cos E} \sin E = \omega_{D_2} \left(\frac{\cos^2 E + \sin^2 E}{\cos E} \right) = \frac{\omega_{D_2}}{\cos E}$$
(B8)

Also from axes set No. 4 and equation (B4)

$$\omega_{\text{E}_4} = \omega_{\text{E}_3} = \omega_{\text{E}_2} \cos A - \omega_{\text{R}_1} \sin A$$
 (B9)

From equations (B3) and (B7)

$$\omega_{R_1} \cos A = \omega_{D_2} \frac{\sin E}{\cos E} - \omega_{E_2} \sin A$$
 (Blo)

$$\omega_{R_{1}} = \left(\frac{\omega_{D_{2}} \sin E}{\cos E \cos A}\right) - \left(\omega_{E_{2}} \frac{\sin A}{\cos A}\right)$$
(B11)

From equations (B9) and (B11)

$$\omega_{\text{E}_4} = \omega_{\text{E}_2} \cos A - \sin A \left(\frac{\omega_{\text{D}_2} \sin E}{\cos E \cos A} - \omega_{\text{E}_2} \frac{\sin A}{\cos A} \right)$$

$$= \omega_{E_2} \left(\frac{\cos^2 A + \sin^2 A}{\cos A} \right) - \omega_{D_2} \left(\frac{\sin A \sin E}{\cos A \cos E} \right)$$
 (Bl2)

From equations (Bl2) and (B8)

$$\omega_{E_4} = \frac{\omega_{E_2}}{\cos A} - \omega_{D_4} \frac{\sin A \sin E}{\cos A} = \frac{\omega_{E_2} - \omega_{D_4} \sin A \sin E}{\cos A}$$
(B13)

Equations (B8) and (B13) give the banked antenna rates in terms of banked control line rates:

$$\omega_{D_4} = \frac{\omega_{D_2}}{\cos E} \tag{B8}$$

$$\omega_{E_4} = \frac{\omega_{E_2} - \omega_{D_4} \sin A \sin E}{\cos A}$$
 (Bl3)

If for convenience we substitute alternate symbols as follows:

$$\omega_{D}^{11} = \omega_{D_{1}}$$

$$\omega_{\rm E}^{\dagger\dagger} = \omega_{\rm E_1}$$

$$\omega_{\mathrm{D}}^{\, \, i} = \omega_{\mathrm{D}}^{\, \, \, \, 2}$$

$$\omega_{\rm E}^{\, t} = \omega_{\rm E}^{\, 2}$$

$$\omega_{\rm D} = \omega_{\rm D_4}$$

$$\omega_{\rm E} = \omega_{\rm E_A}$$

the following definitions result:

 ω_D " = programmed azimuth rate about unbanked control line axes

 $\omega_{\rm E}$ " = programmed elevation rate about unbanked control line axes

 $\omega_{\mathrm{D}}^{\,\, t}$ = azimuth rate about banked control line axes

 $\omega_{\mathbb{R}}$! = elevation rate about banked control line axes

 ω_{D} = azimuth rate about banked antenna axes

 $\omega_{\mathbb{R}}$ = elevation rate about banked antenna axes

Thus the computer is required to perform the functions illustrated in figure 13.

It may be noted that the transformation equations are based on rates about an assumed control line. In practice, the antenna A and E angles are measured from the airplane center line; hence, the transformations will be affected if the aircraft deviates from the chosen control line. Nevertheless, the transformation performs the essential function of converting the rates to banked antenna axes and any resultant inaccuracies were accepted as part of the price of simplicity.

Mechanization of Axes Transformation Computer

The axes-transformation computer operates as indicated by figure 13. The two programmed rate signals ω_D " and ω_E " are supplied by the camdriven linear transformers. These signals pass through a roll resolver, mounted on a gyro measuring airplane bank angle, which transforms them from unbanked to banked axes rates ω_D ' and ω_E '. The signals then pass through feedback amplifiers which have resolvers in the feedback loop, thus dividing the rate signals by the cosine of the resolver angle. The output of the axes transformation computer consists of two voltages which are proportional to the desired rates in terms of banked antenna axes. These voltages are supplied to the E-4 torque-current amplifier, as shown in figure 6, to produce a torque in each of the HIGU gyros. This causes the antenna to be driven at the desired rate.

APPENDIX C

PROGRAM LAYOUT AND ASSOCIATED EQUATIONS

Fundamental Attack Courses

To compute a simulated attack program properly for a system such as the E-4, it is essential that the program be constructed on the basis of the flight geometry used in the associated fire-control system computer. To orient the reader, it might be well to review briefly four variations of attack courses commonly used in air-to-air combat. These are the pursuit course, the lead pursuit course, the collision course, and the lead-collision course.

The pursuit course is one in which the pilot flies directly at the target at all times; consequently, no provision is made for leading the target to allow for armament travel time.

The lead pursuit is a modified pursuit course in which the attacker flies with a lead angle, that is, flies toward a point some distance ahead of the target. A proper lead angle allows the armament to be fired at any point during the attack, once within armament range. This attack course is used for armament requiring long firing times, such as machine guns.

In a collision course, figure 14, the attacker flies toward a point where the target and attacker will arrive at the same time. If the target path and speed do not change and the attacker speed is constant, the attacker path is a straight line toward a fixed collision point; furthermore, the bearing of the target relative to the attacker is a constant angle.

The lead-collision course, figure 15, such as used in the Hughes E-4 fire-control system, is a straight line course having a fixed lead angle from the straight collision course. This type of course requires the attacker to be in position at only one instant - that at which the armament is fired.

Basic E-4 Steering Equations

Since the E-4 system is based on the lead-collision course, an understanding of the steering equations associated with this type of course is essential to an understanding of the programming details. References 2 and 4 give a detailed explanation, from which the following pertinent information has been extracted.

An examination of figures 16(a) and 16(b) discloses the attack pattern, in space coordinates, under conditions of a hit and a miss. In T seconds the target and attacker travel V_BT yards and V_AT yards along their respective courses. The rockets, when fired, travel at a velocity V_R which is greater than V_A ; therefore, after t seconds the rocket travel will be V_R t and the attacker travel will be V_A t. The difference in distance after t seconds is the relative rocket travel, a fixed distance for a fixed firing time t, and may be considered as a pole F yards long projecting ahead of the attacker. The problem, then, is to fly the end of this F pole into the target.

Since the radar makes its measurements relative to the attacker, the flight geometry is based on target and rocket motion relative to the attacker. Consider the two-dimensional case, figure 17, where all the quantities are measured relative to the attacker. The "miss" may be resolved into two components. One along the line of sight ($M_{\rm LS}$) and one perpendicular to the line of sight ($M_{\rm horz}$). Two steering equations are obtained by equating these miss components to zero.

Examination of figure 17 shows that the miss component along the line of sight can be represented by the following equation:

$$M_{LS} = R + RT - F \cos(-A)$$

Signs are chosen to match convention used in the E-4 technical order. (Note that range is decreasing, making \mathring{R} negative.) For zero miss:

$$R + RT - F \cos(-A) = 0$$

This is the time equation solved by the computer, and on the basis of this T, the attacker must change course to reduce the horizontal miss to zero. Further examination of figure 17 shows that the horizontal miss is defined by the following equation:

$$M_{horz} = R\omega_D T - F_{sin}(-A)$$

or for zero miss (horz)

$$R\omega_DT - F_{sin}(-A) = 0$$

Extension of the equations to cover the three-dimensional case, based on the geometry of figure 18 from reference 2, results in somewhat modified equations as follows:

Time

$$R + \hat{R}T - F \cos A \cos E = 0$$

Horizontal steering

$$R\omega_D + \frac{F}{T} \sin A = 0$$

Elevation steering, which is complicated by the rocket ballistics, may be written in a simplified form as follows:

$$R\omega_{E}$$
 + $\frac{F}{T}$ cos A sin E + $\frac{F}{T}$ (ballistics terms) = 0

Program Computation

The program used for the Ames E-4 target simulator was computed by starting with the point of impact and working backward in time; in addition, it was assumed that the target flew a straight path. Attacker approaches were calculated from 120°, 90°, and 60° angles with respect to the bomber path. This gave the three runs illustrated by figure 19.

The attacker was given a 5-percent speed advantage, with the attacker velocity taken to be 271 yards per second and the target velocity set at 258 yards per second. These conditions correspond to a Mach number of 0.8 at 25,000 feet altitude for the attacker.

Program layout to 20 seconds or 5000 yards. The bomber flight path was laid out to scale by plotting the position points backward from the impact point, allowing 258 yards for each second of run.

Because of the relative rocket travel distance, "F" being 500 yards, the initial point (at time-to-go, T equal to zero) of the attacker flight path was plotted 500 yards from the point of impact, at the assumed bearing. From this point back to T equal to 20 seconds or to where the range equaled 5000 yards, whichever occurred first, the same procedure was used for the attacker flight path as was used for the target, with the exception of allowing 271 yards traveled per second for attacker velocity. The procedure used past the mentioned T and range limits will be discussed later.

The resultant target and attacker flight path plot, in space coordinates, was used to determine the range, R, and angle, A, at each second

of time-to-go. From these measured quantities, the angular line-of-sight rate, ω_D , and the range-rate, \dot{R} , were computed by use of the time-to-go and the horizontal steering equations.

Equations used for conditions past 20 seconds or 5000 yards. As a result of E-4 mechanization limitations, a new relationship exists between the attacker-target flight geometry and the computer equations for T greater than 20 seconds and range greater than 5000 yards. This new relationship may be developed from figure 20 by setting up equations based on both the flight path geometry and the computer equations using the limited quantities.

The angle -A shown in figure 20(a) is the line-of-sight angle with respect to attacker longitudinal axis. It was not used in connection with the calculation of the program for T less than 20 seconds and R less than 5000 yards but must be considered for calculation of the flight path for T greater than 20 seconds and R greater than 5000 yards. The value of range used by the E-4 computer servo is designated by R_{servo}; it cannot exceed 5000 yards. The actual range is designated by R_{actual}. For R_{actual} less than 5000, R_{servo} equals R_{actual}, and for R_{actual} greater than 5000, R_{servo} equals 5000. Similarly, the symbol T_{lim} is used to designate the value of time-to-go used by the E-4 computer; it cannot exceed 20 seconds. For T less than 20, T_{lim} equals T, and for T greater than 20, T_{lim} equals 20. From the geometry of figure 20(a):

$$R_{actual} \omega_{D}T = F \sin(-A)$$
 (C1)

However, the computer uses the values $\,R_{\hbox{\scriptsize servo}}$ and $T_{\hbox{\scriptsize lim}}\,$ in processing this equation; consequently,

$$R_{\text{servo}} \omega_{\text{D}} T_{\text{lim}} = F \sin(-A)$$
 (C2)

Also, from figure 20(b)

$$\omega_{\rm D} = \frac{V_{\rm B} \sin B - V_{\rm A} \sin(-A)}{R_{\rm actual}}$$
 (C3)

where

VB target velocity

V_A interceptor velocity

B relative bearing of attacker from bomber path

The radar measures this actual rate, so the R_{actual} term is used. Now substituting equation (C3) into equation (C2):

$$R_{\text{servo}} \left[\frac{V_{\text{B}} \sin B - V_{\text{A}} \sin(-A)}{R_{\text{actual}}} \right] T_{\text{lim}} = F \sin(-A)$$
 (C4)

and solving for sin(-A):

$$\sin(-A) = \frac{V_B \sin B}{V_A + \frac{F}{T_{lim}} \left(\frac{R_{actual}}{R_{servo}}\right)}$$
 (C5)

This equation is always satisfied by the E-4 computer and the flight geometry. It could have been used in computing the attacker path for the unlimited case ($R_{\tt Servo} = R_{\tt actual}$ and $T_{\tt lim} = T$) but, historically, the graphical procedure previously discussed was developed earlier and was used for many early calculations that were not carried beyond the computer limits of R and T. When the calculation of the limited case was finally faced, it was not deemed necessary to recompute the unlimited part of the path merely for the sake of consistency. Equation (C5) must be used when plotting the attacker path beyond the limit of either the time or range servos.

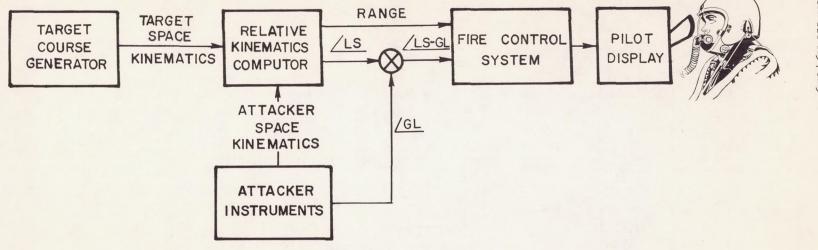
Discussion of limited case calculations .- The calculations for the conditions where T was less than 20 seconds and R was less than 5000 yards, were made point by point starting with point 0, figure 19, where T = O and R = F. As these calculations were made for succeeding points, both R and T increased until at some point (number n, fig. 21) the above limitations were approached so closely that upon calculating the conditions at point n + 1, it was found that either R_{n+1} was greater than 5000 or T_{n+1} was greater than 20. It was then necessary to go back to the conditions at point n and use equation (C5) to arrive at point n + 1. During the part of the run that the unlimited conditions existed, the attacker path was a straight line; therefore, the flight path angle, \(\lambda\), was the same for each point. For the limited part of the path, the attacker path is no longer a straight line and the angle λ will change from point to point. However, this change will be small and the n + l point can be calculated by assuming that $\lambda_{n+1} = \lambda_n$ and then calculating R_{n+1} , \dot{R}_{n+1} , and $\omega_{D_{n+1}}$ by straight trigonometry. These values can then be used to find what λ_{n+1} should have been. Call this quantity λ^{\bullet}_{n+1} . This modified value, $\tilde{\lambda}^{\bullet}_{n+1}$, was not used in connection with point n+1 since, as pointed out, the change is slight; however, it was used to compute point n + 2. The assumption can then be made that

the calculated value of λ^{\bullet}_{n+1} is the same as λ_{n+2} and the process discussed above can be repeated to calculate point n+2. The above procedure is repeated until the desired number of positions are obtained. It may be of interest to note that no scale plot of the run is needed for the limited servo case procedure; however, such a plot is useful for checking purposes.

At the very beginning of each run, a 4-second, straight portion, followed by a 3° per second turn for 5 seconds was injected into the program for realistic effects. This was accomplished, when working backwards, by varying λ 3° per second for 5 seconds and then keeping it constant for the next 4 seconds.

REFERENCES

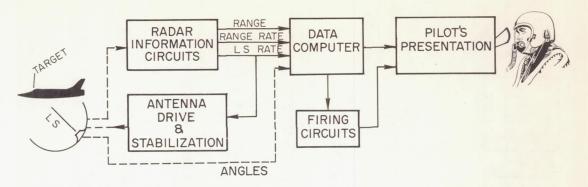
- 1. Doolin, Brian F., Smith, G. Allan, and Drinkwater, Fred J., III: An Air-Borne Target Simulator for Use in Optical-Sight Tracking Studies. NACA RM A55F20, 1955.
- 2. Anon.: Handbook Service Instructions, Fire Control System Type E-4. U.S.A.F. Tech. Order No. 11F1-E4-2, 16 Feb. 1954.
- 3. Jarosh, J. J.,: Single-Degree-of-Freedom Integrating Gyro Units for Use in Geometrical Stabilization Systems. Rep. No. 6398-S-11, M.I.T. Inst. Lab., Mar. 1950.
- 4. Anon.: An Electronic Rocket-Fire Control Computer. Tech. Memo. No. 238, Hughes Aircraft Company, July 1, 1950.



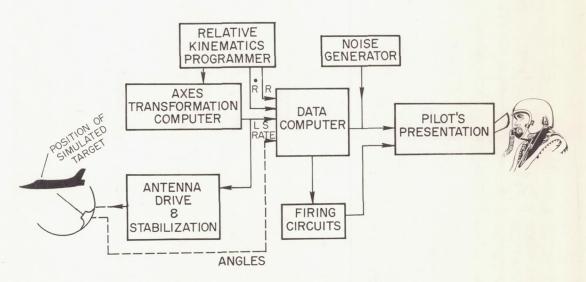
GL IS ANGLE BETWEEN ATTACKER GUNSIGHT LINE AND A FIXED SPACE AXIS.

LS IS ANGLE BETWEEN ATTACKER LINE OF SIGHT TO TARGET AND A FIXED SPACE AXIS.

Figure 1.- Simplified diagram of general purpose target simulator which was investigated but not built.



(a) NORMAL E-4 SYSTEM



(b) TARGET SIMULATOR COMPONENTS ADDED

Figure 2.- Functional block diagram of E-4 system with and without target simulator.

NACA RM A57C19 31

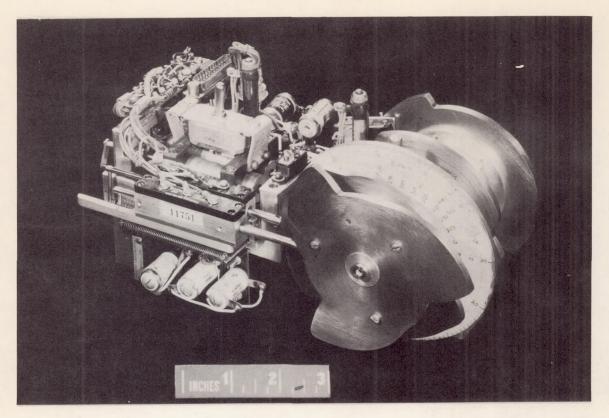


Figure 3.- Target simulator programmer.

A-21055

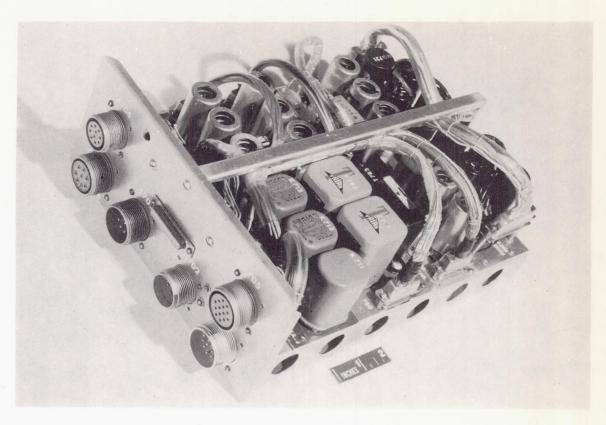


Figure 4.- Axes transformation computer.

A-19108



Figure 5.- Target simulator noise generator.

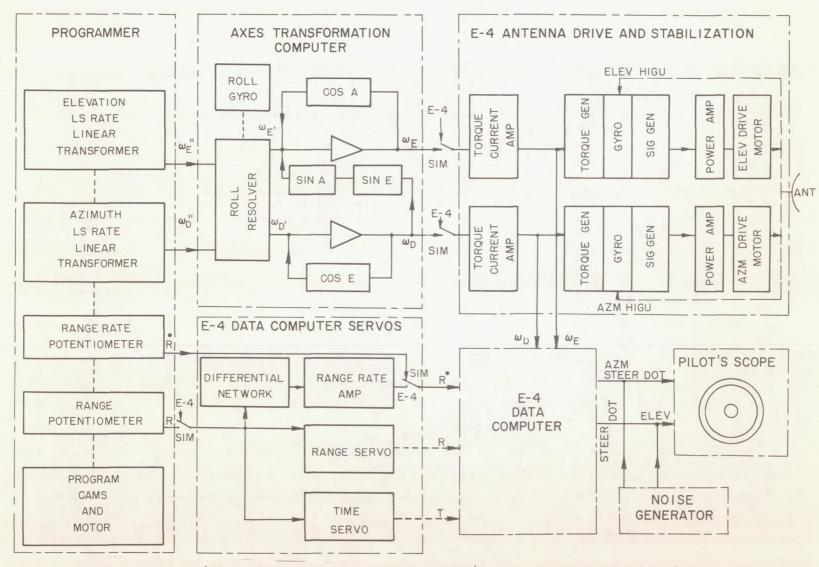


Figure 6.- Simplified block diagram of E-4 system with target simulator.

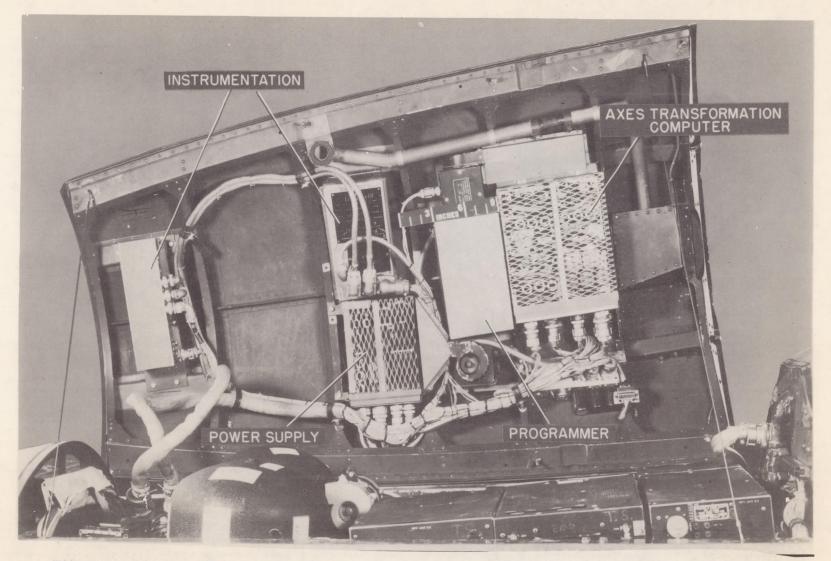


Figure 7.- Target simulator equipment installed in nose hatch cover of test airplane.

A-Zuou.

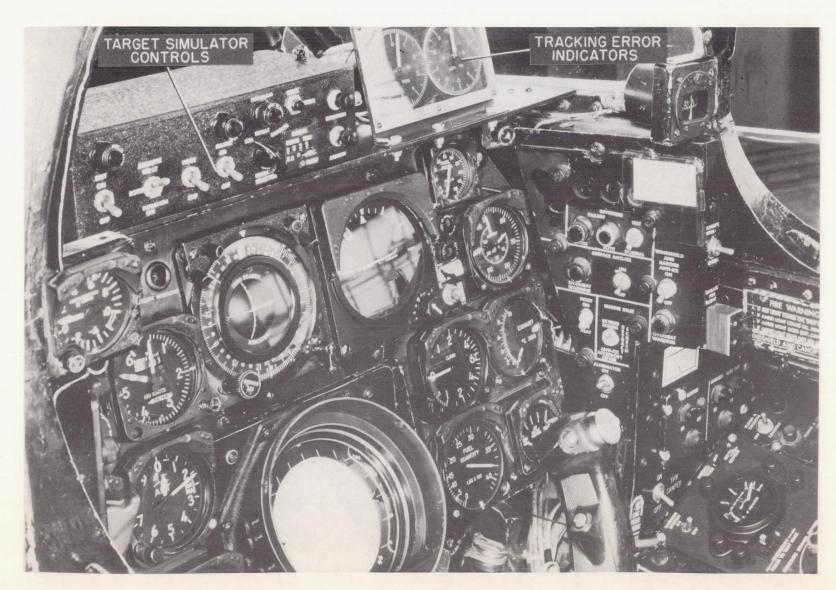
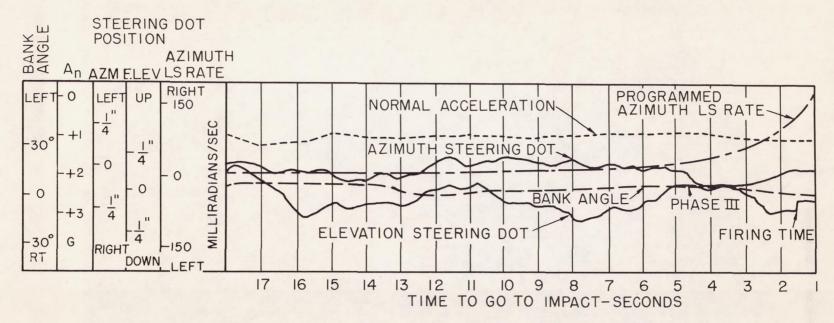


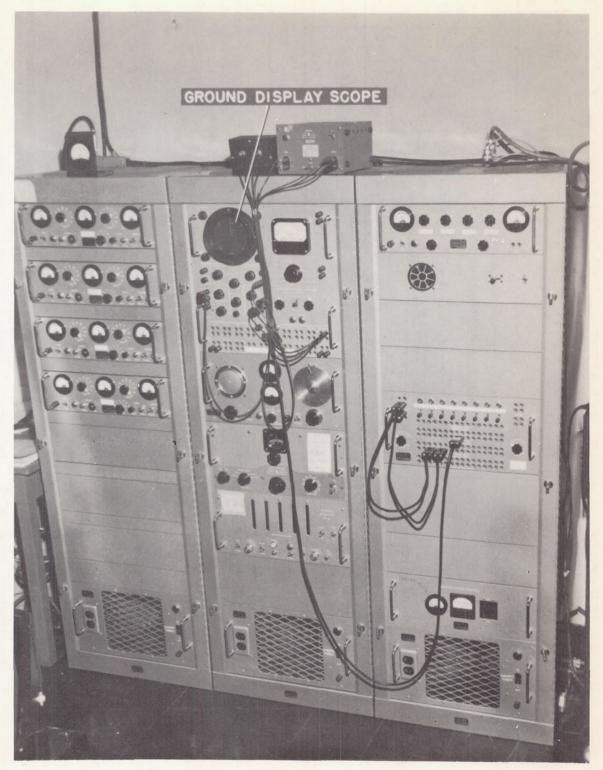
Figure 8.- Cockpit view of test airplane showing simulator controls.

A-20337.2



NOTE: 1 STEERING DOT MOTION EQUALS REFERENCE CIRCLE DIAMETER

Figure 9.- Time history during latter part of typical attack.



A-20555.2

Figure 10.- Telemeter ground station showing ground display scope.

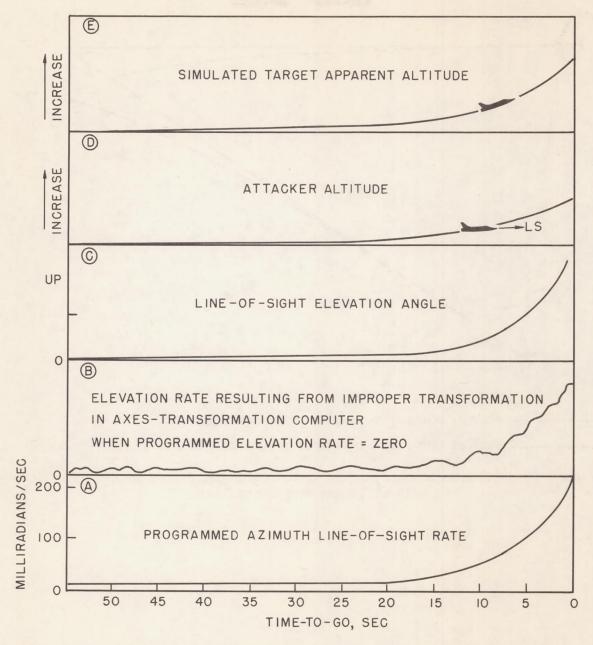
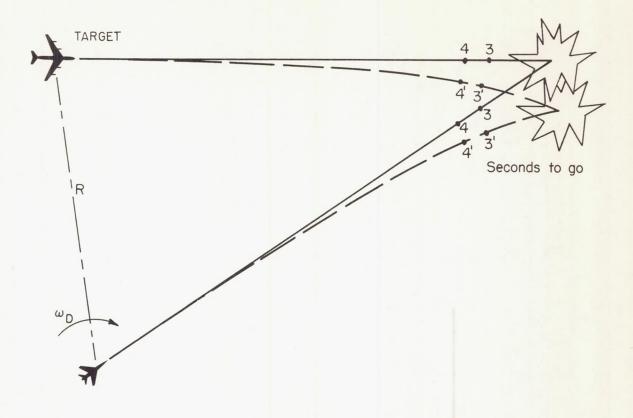


Figure 11.- Effects of improper elevation line-of-sight rate resulting from improper axes transformation computation. (NOTE: A results in B, which results in C, etc.; not to scale.)



Path resulting from properly programmed quantities
 Path resulting from quantities programmed in an improper relationship

Figure 12.- Illustration of curved path resulting from improper relationship of programmed quantities.

D

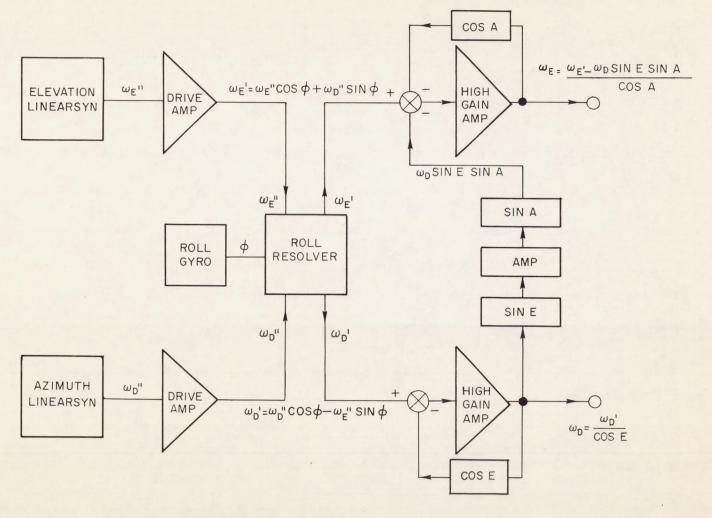


Figure 13.- Axes-transformation computer.

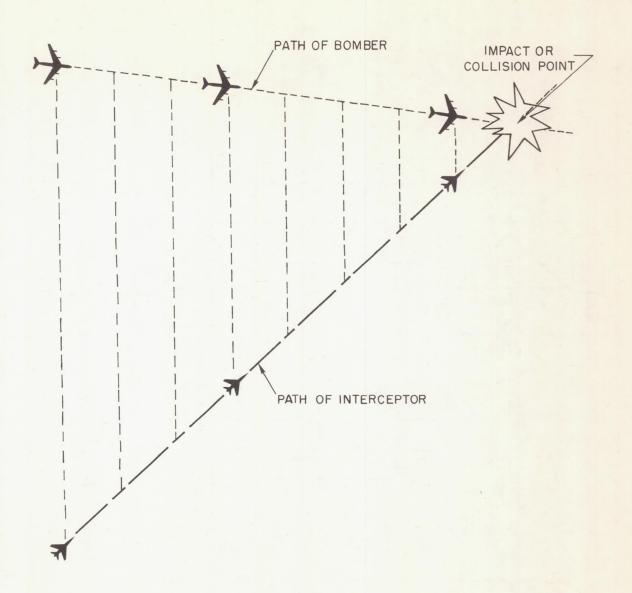


Figure 14.- Collision course.

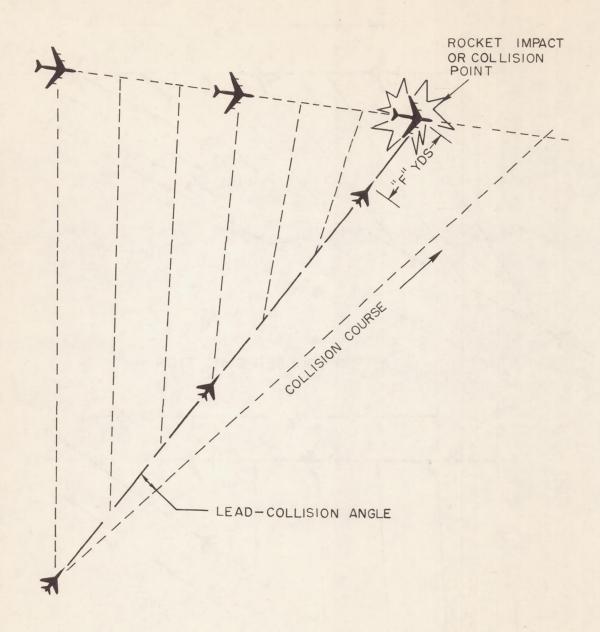


Figure 15.- Lead-collision course.

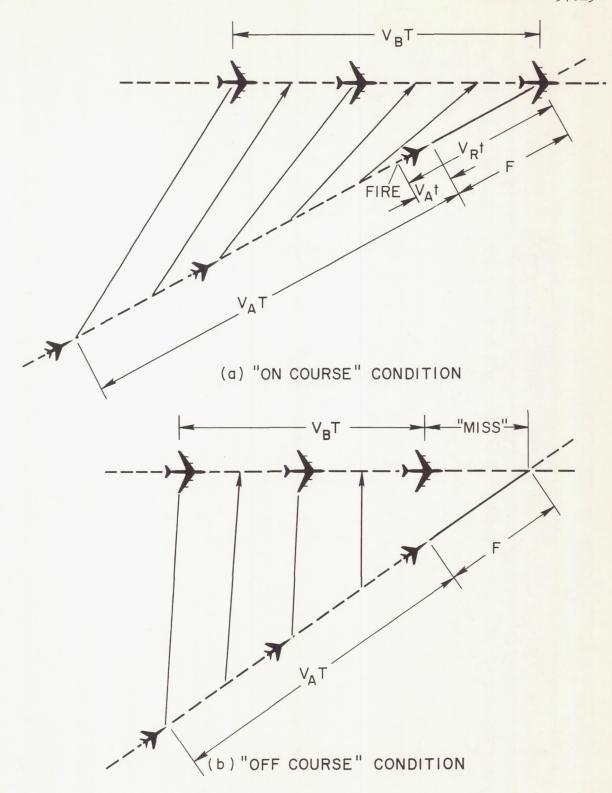


Figure 16.- Lead-collision course conditions.

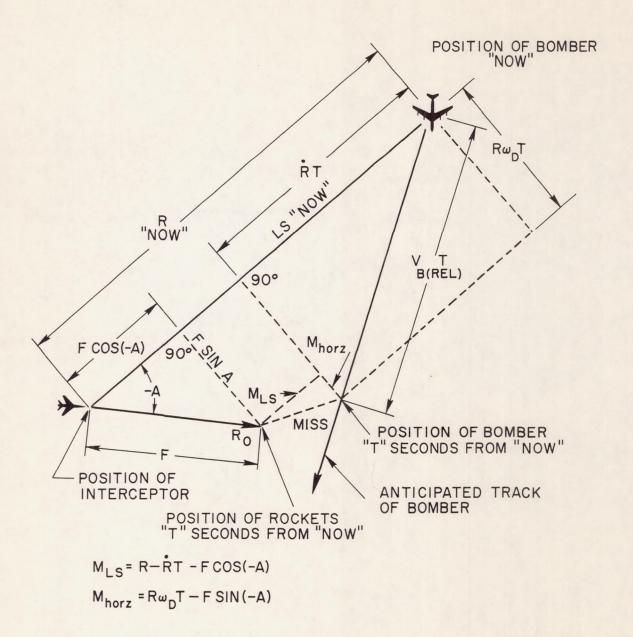


Figure 17.- Fire-control problem in relative coordinates.

AZIMUTH STEERING $R\omega_D + \frac{F}{T}SINA=0$

ELEVATION STEERING $R\omega_E + \frac{F}{T}\cos A \sin E = 0$

TIME EQUATION R+RT - F COS A COSE = O

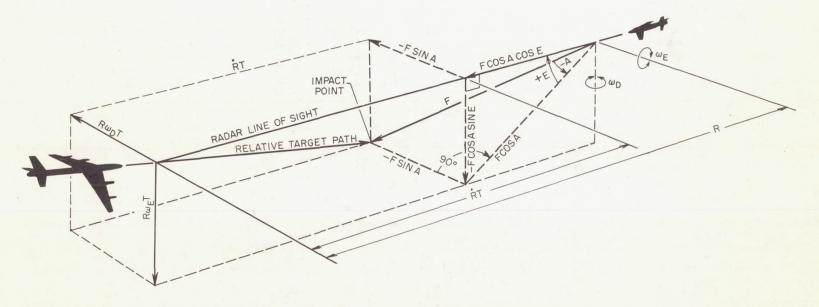


Figure 18.- The E-4 steering geometry.

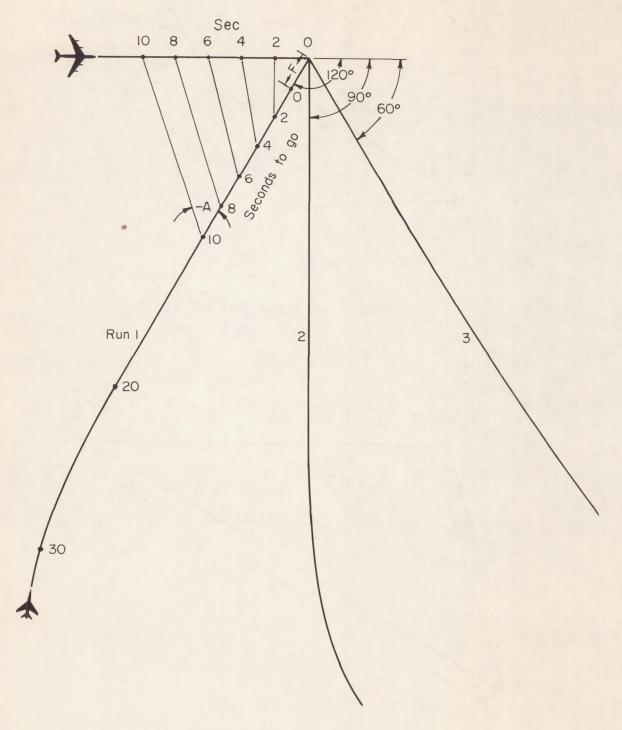
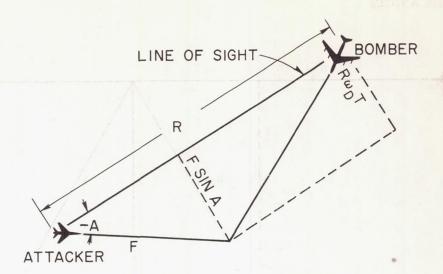
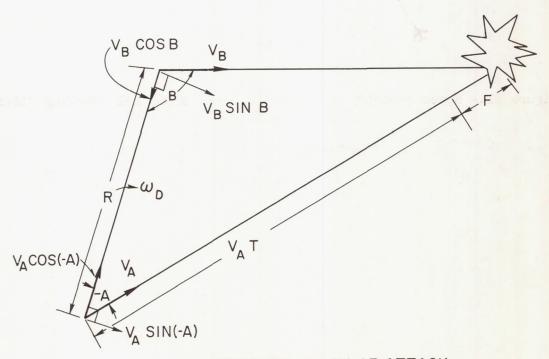


Figure 19.- Typical program attack patterns.



(a) RELATIVE GEOMETRY OF ATTACK



(b) SPACE GEOMETRY OF ATTACK

Figure 20.- Attack geometry.

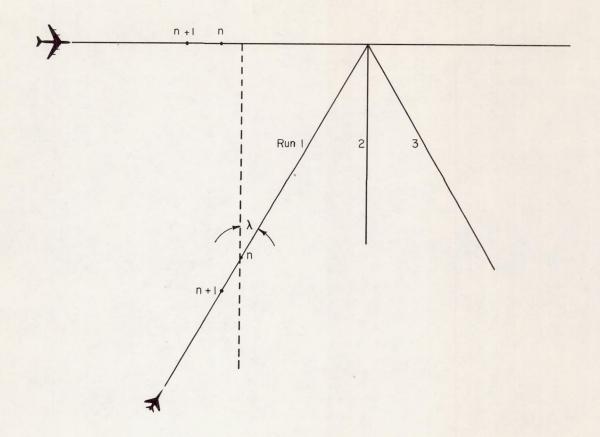


Figure 21.- Space geometry of attack at time $\,$ n and n+l $\,$ showing flight-path angle $\,\lambda\,.$